PROCEEDINGS OF SCIENCE

Measurements of the Longitudinal Proton Structure Function F_L at HERA

Burkard Reisert[*†]
Max-Planck-Institut für Physik, Föhringer Ring 6, 80805 München, Germany
E-mail: reisert@mppmu.mpg.de

The measurements of the longitudinal proton structure function F_L in deep inelastic positron-proton scattering at low Bjorken x are presented. The data were taken by the HERA experiments H1 and ZEUS in a series of runs with different proton beam energies. The measured longitudinal structure function is compared to theoretical predictions in higher order QCD and using dipole model calculations.

The 2009 Europhysics Conference on High Energy Physics,
July 16 - 22 2009
Krakow, Poland

[*]Speaker.
[†]Presentation on behalf of the H1 and ZEUS collaborations [1]

PoS(EPS-HEP 2009)309

1. Deep Inelastic Scattering Cross Sections and Structure Functions

The inclusive deep inelastic (DIS) neutral current (NC) positron-proton scattering cross section at low negative four-momentum transferred squared, Q^2, can be written in its reduced form as

$$\sigma_r(x,Q^2,y) = \frac{d^2\sigma}{dxdQ^2}\cdot\frac{Q^4x}{2\pi\alpha[1+(1-y)^2]} = F_2(x,Q^2) - \frac{y^2}{1+(1-y)^2}F_L(x,Q^2). \qquad (1.1)$$

Here, α denotes the fine structure constant, x is the Bjorken scaling variable representing the momentum fraction of the proton carried by the scattered parton, and y is the inelasticity of the scattering process. The cross section is determined by two independent structure functions, F_2 and F_L. They are related to the $\gamma^* p$ absorption cross sections of longitudinally and transversely polarised virtual photons, σ_L and σ_T, according to $F_2 \propto (\sigma_L + \sigma_T)$ and $F_L \propto \sigma_L$, therefore $0 \leq F_L \leq F_2$. The structure function F_2 is the sum of the quarks and anti-quarks x distributions weighted by the electric charges of the quarks squared and is the dominating contribution to the cross section. In the Quark Parton Model the value of the longitudinal structure function F_L is zero, whereas in Quantum Chromodynamics (QCD) F_L differs from zero due to the presence of gluons in the proton.

Information about F_L at large x had been obtained by a number of fixed target lepton-proton scattering experiments [2], beginning with the discovery at SLAC that the ratio $R \simeq F_L/(F_2 - F_L)$ was close to zero which was a most convincing evidence for the quarks to be spin $1/2$ fermions. The measurement of F_L at HERA constitutes the first-ever direct determination of F_L in the kinematic region of low Bjorken x and therefore it has since long been recognised as an important part of the HERA programme [3].

Indirect measurements of F_L by H1 [4, 5, 6], which were relying on an extrapolated F_2 at low x, did hint to larger values of the longitudinal proton structure function at low x. This is to be expected as F_L at low x is dominated by the contribution of the gluon which rises steeply as x decreases. While R at large x is a measure of the quark spin, at low x it rather quantifies the dynamics of the gluon interactions and as such is of particular theoretical interest [7].

2. Ingredients to the Measurement of F_L

As evident from Eq. 1.1, the structure functions F_2 and F_L at fixed x and Q^2 can be extracted in a model independent way by fitting a straight line to the values of σ_r plotted against $y^2/[1+(1-y)^2]$ in the so-called Rosenbluth plot, see Fig. 1 for an example. The intercept at $y^2/[1+(1-y)^2] = 0$ represents $F_2(x,Q^2)$ while the value of F_L is implied by the slope of the straight line.

The kinematic variables x, Q^2 and y are related by $y = \frac{Q^2}{x\cdot s}$ with $s = 4E_eE_p$ being the positron-proton centre-of-mass energy. Therefore varying y – while keeping x and Q^2 constant – requires to vary s. At HERA the variation of s was achieved by lowering the proton energy E_p while keeping the electron energy $E_e = 27.5\,\text{GeV}$ constant.

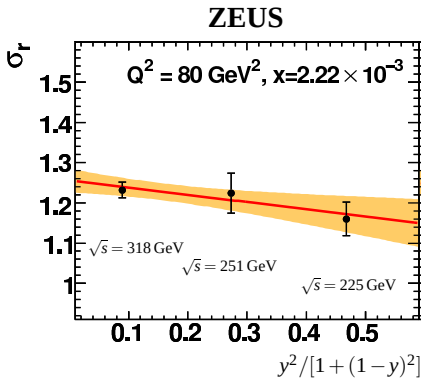

Figure 1: Example of the reduced cross section at fixed x and Q^2 as a function of $y^2/[1+(1-y)^2]$. The line and band indicate the central value and uncertainty of the linear fit to extract F_2 and F_L [17].

The precision of the determination of F_L crucially depends on the range available in $y^2/[1+(1-y)^2]$. This was maximised by collecting data at the nominal HERA energy $E_p = 920\,\text{GeV}$, $\sqrt{s} = 318\,\text{GeV}$ (high energy run, HER) and at $E_p = 460\,\text{GeV}$, $\sqrt{s} = 225\,\text{GeV}$ (low energy run, LER) the lowest attainable energy with adequate instantaneous luminosity which decreases $\propto E_p^2$ and stable beam orbits within the limited aperture of the HERA proton ring. An intermediate data set was collected at $E_p = 575\,\text{GeV}$, $\sqrt{s} = 251\,\text{GeV}$ (medium energy run, MER) achieving approximately equidistant separation of the measurements in $y^2/[1+(1-y)^2]$.

The sensitivity to F_L is largest at high y as its contribution to σ_r is proportional to y^2. The kinematic variables y, Q^2 and x are determined from the energy, E'_e, and polar angle, θ_e, of the scattered electron:

$$y = 1 - \frac{E'_e}{2E_e}(1-\cos\theta_e),\ Q^2 = 2E'_eE_e(1+\cos\theta_e),\ x = \frac{Q^2}{sy}. \tag{2.1}$$

If therefore one intends to measure σ_r at high y one needs to master the trigger rate and electron identification at small energies of a few GeV. Such energies are deposited much more frequently by hadrons from photoproduction (γp) processes, for which $Q^2 \simeq 0$, than by genuine scattered positrons.

Removal of the γp background constitutes the major challenge of the measurement of F_L at HERA. There are two ways to control the γp background: part of the γp events is uniquely identified by detecting the scattered positron near to the beam axis in tagging calorimeters downstream the e^+ beam. That measurement can be used to tune the Monte Carlo simulation of the background. In a further method the charge symmetry of the background is used. While a DIS positron carries the lepton-beam charge, energy deposits due to hadrons from γp processes are charge symmetric, apart from a small proton-antiproton cross-section difference one can correct for. With tracking detectors in front of the calorimeters the charge of the DIS lepton candidate can be determined and the wrong charge signal can be statistically subtracted. ZEUS has subtracted the background with a tagger based simulation, for $E'_e > 6\,\text{GeV}$, in which subprocesses simulated by the PYTHIA Monte Carlo program are weighted using ZEUS γp cross section data. H1 has primarily used the charge measurement.

3. Results: NC Cross Section and Structure Functions

The ZEUS collaboration has recently published [8] neutral current cross sections for medium Q^2, $20 < Q^2 < 130\,\text{GeV}^2$ and $0.09 < y < 0.78$ using data sets of $44.5\,\text{pb}^{-1}$, $7.1\,\text{pb}^{-1}$ and $13.9\,\text{pb}^{-1}$ for the HER, MER and LER analyses. The cross sections are shown in Fig. 2 (left) as a function of x for fixed Q^2. The cross sections from the HER period constitute the most precise measurement by ZEUS in the measured range. The extracted values of F_2 and F_L are displayed in Fig. 2 (right). The measurement of F_2 is the first-ever model-independent determination of F_2 at low x. The measurement of F_L is clearly different from zero and is well described by the next-to-leading-order (NLO) prediction based on the PDFs from the ZEUS-JETS fit [9]. From a combination of the measurements at a given Q^2 the structure function F_L and the ratio $R = F_L/(F_2 - F_L)$ are extracted as a function of Q^2. For the Q^2 range covered, 20 to $130\,\text{GeV}^2$, ZEUS quotes an average value of $R = 0.18^{+0.07}_{-0.05}$. Figure 4 shows a comparison of these measurements with predictions based on the

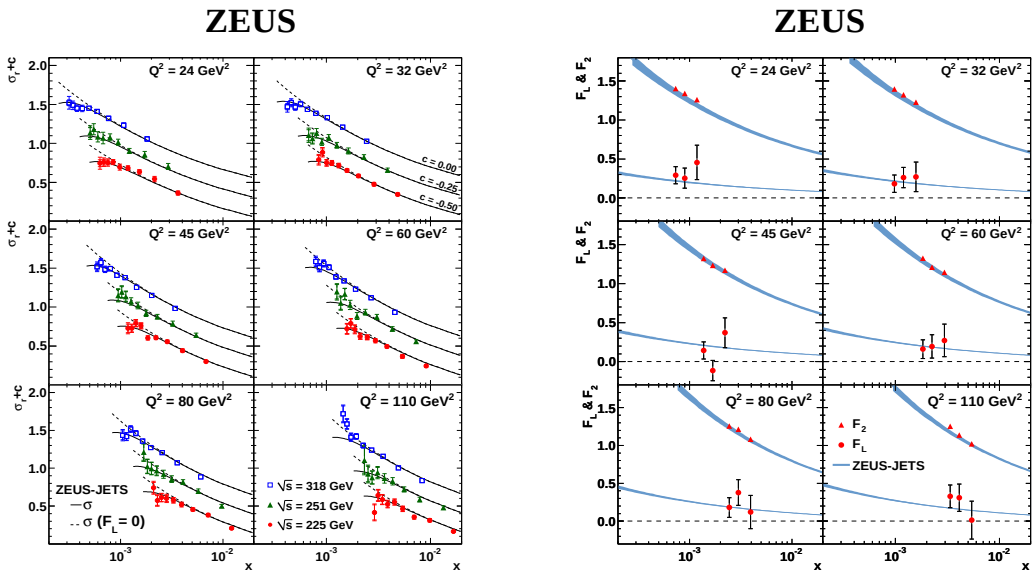

Figure 2: The measured cross sections for $\sqrt{s} = 318,\ 251$ and 225 GeV (left) and the extracted structure functions F_2 and F_L (left) as a functions x for fixed values of Q^2 from the ZEUS analysis. The measurements are compared to a NLO calculation based on the ZEUS-JETS PDFs [9].

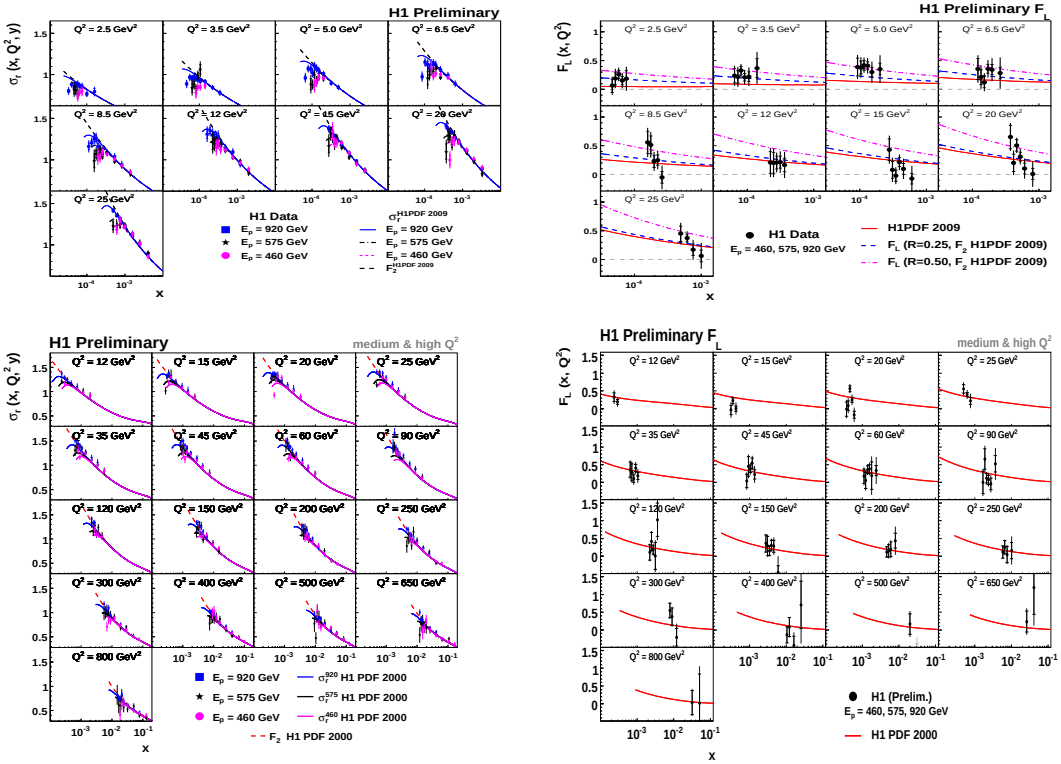

Figure 3: The measured cross sections for $E_p = 920,\ 575$ and 460 GeV (left) and the extracted structure function F_L (right) as a functions x for fixed values of Q^2 from the H1 low Q^2 (top) and H1 medium&high Q^2 analyses (bottom). The measurements are compared to a NLO calculation based on the H1 PDF 2009 [18] and H1 PDF 2000 PDFs [6].

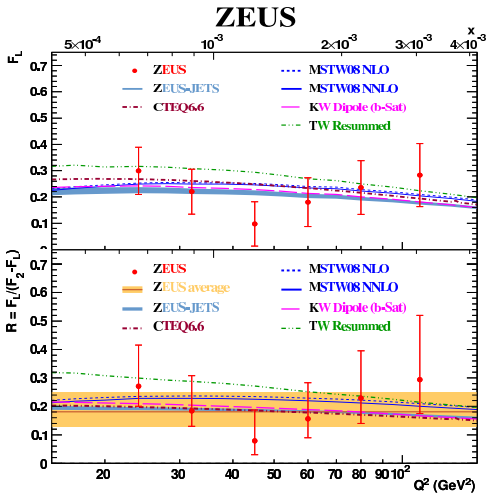

Figure 4: Values of averaged F_L (top) and $R = F_L/(F_2 - F_L)$ (bottom) as a function of Q^2. The shaded band represents the 68% probability interval for the overall averaged R. The lines represent various model predictions.

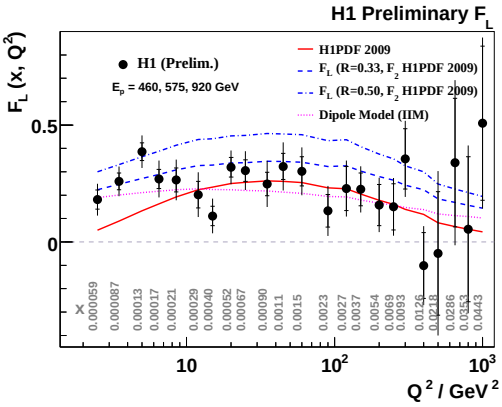

Figure 5: The measured $F_L(Q^2)$ averaged in x at given values of Q^2. The resulting x values of the averaged F_L are given in the figure for each point in Q^2. The curves represent the predictions of a dipole model as well as of perturbative QCD calculation at NLO using the H1 PDF 2009.

ZEUS-JETS and CTEQ6.6 [10] NLO as well as MSTW08 [11] NLO and NNLO fits. All these predictions are based on the DGLAP formalism. Also shown are predictions from the NLL BFKL resummation fit from Thorne and White (TW) [12] and the prediction from the impact-parameter-dependent dipole saturation model (b-Sat) of Kowalski and Watt based on the DGLAP evolution of the gluon density [13]. All the models are consistent with the data.

The H1 results are based on data sets of $21.6\,\mathrm{pb}^{-1}$ (HER), $6.2\,\mathrm{pb}^{-1}$ (MER) and $12.4\,\mathrm{pb}^{-1}$ (LER). The H1 analyses profited from the continued efforts to improve the backward calorimetry and tracking systems as well as from various trigger upgrades to enhance the trigger efficiency of low energy electrons. This enables H1 to measure the scattered electron at an energy as low as 3 GeV, while using the charge measurement of the track associated with the electron candidate to control the background. H1 have extended their published measurement [14] towards high Q^2, up to $800\,\mathrm{GeV}^2$, and low Q^2, down to $2.5\,\mathrm{GeV}^2$, and obtain values of F_L at up to 6 different values of x at a given Q^2. Figure 3 shows σ_r (left) and extracted F_L (right) as a function of x at fixed values of Q^2. F_L averaged over x as a function of Q^2 is shown in Fig. 5. For $Q^2 > 10\,\mathrm{GeV}^2$, the measurement is well described by NLO predictions, whereas at lower Q^2 the perturbative QCD calculation underestimates the measurement. Dipole models [15, 16] are found to describe the data well. For the entire Q^2-range the measurement is consistent with a value of $R = 0.25$.

4. Summary

Both HERA collider experiments H1 and ZEUS have published direct measurements of the longitudinal proton structure function at medium Q^2 probing the gluon-dominated low x regime. H1 succeeded to significantly extend the Q^2 range of their measurement. At low x and not too small Q^2 the prediction of F_L relies nearly completely on the behaviour of the gluon distribution, which is determined at low x from the scaling violations of $F_2(x, Q^2)$. The consistency of the theoretical calculation on F_L with the data above $Q^2 \simeq 10\,\mathrm{GeV}^2$ is therefore a non-trivial test of QCD to high orders.

Acknowledgments

The measurement of F_L became possible thanks to the engagement and competence of the HERA machine crew. The understanding of the machine had reached the most impressive level, as became clear during the low and medium energy run when the optics, the polarisation, the instantaneous luminosity and the overall operation efficiency were all up to or even beyond expectations. The continued support of the collider experiments H1 and ZEUS by the DESY directorate after the termination of the operation of HERA has been – and still is – vital to the completion of the analyses.

References

[1] URL to the slides of the presentation at EPS09: `http://indico.ifj.edu.pl/MaKaC/contributionDisplay.py?contribId=990&sessionId=22&confId=11`

[2] EMC Collaboration, J.J. Aubert *et al.*, Phys. Lett. **B121**, 87 (1983);
BCDMS Collaboration, A.C. Benvenuti *et al.*, Phys. Lett. **B223**, 485 (1989);
L.W. Whitlow *et al.*, Phys. Lett. **B250** 193 (1990);
NMC Collaboration, M. Arneodo *et al.*, Nucl. Phys.**B483**, 3 (1997).

[3] A.M. Cooper-Sarkar *et al.*, Z. Phys. **C39**, 28 (1988), also HERA Workshop 1987, Proceedings Vol 1, p.231; J.Blümlein *et al.* PHE-88-01, Vol 1, p.67, Hamburg 1987, ed. R.Peccei.

[4] H1 Collaboration, C. Adloff *et al.*, Phys. Lett. **B393** 452 (1997) [arXiv:9611017 [hep-ex]].

[5] H1 Collaboration, C. Adloff *et al.*, Eur. Phys. J. **C21** 33 (2001) [arXiv:0012053 [hep-ex]].

[6] H1 Collaboration, C. Adloff *et al.*, Eur. Phys. J. **C30**, 1 (2003) [arXiv:0304003 [hep-ex]].

[7] For example see: J. Blümlein *et al.*, Nucl. Phys. **B755**, 272 (2006);
A.D. Martin, W.J. Stirling and R.S. Thorne, Phys. Lett. **B635**, 305 (2006).

[8] ZEUS Collaboration, S. Chekanov it et al., submitted to Phys. Lett. B, arXiv:0904.1092 [hep-ex].

[9] ZEUS Collaboration, S. Chekanov *et al.*, Eur. Phys. J. bf C42, 1 (2005) [arXiv:0503274 [hep-ph]].

[10] P.M. Nadolsky *et al.*, Phys. Rev. **D78**, 013004 (2008) [arXiv:0802.0007 [hep-ph]].

[11] A.D. Martin *et al.*, Submitted to Eur. Phys. J. C, arXiv:0901.0002 [hep-ph].

[12] C.D. White and R.S. Thorne, Phys. Rev. **D75**, 034005 (2007) [arXiv:0611204 [hep-ph]].

[13] G. Watt and H. Kowalski, Phys. Rev. **D78**, 014016 (2008) [arXiv:0712.2670 [hep-ph]].

[14] H1 Collaboration, F.D. Aaron *et al.*, Phys. Lett. **B665**, 139 (2008) [[arXiv:0805.2809 [hep-ex]].

[15] K. Golec-Biernat and M. Wüsthoff, Phys. Rev. **D59**, 014017 (1999) [arXiv:9807513 [hep-ph]].

[16] E. Iancu, K. Itakura and S. Munier, Phys. Lett. **B590**, 199 (2004) [arXiv:0310338 [hep-ph]].

[17] `http://www-zeus.desy.de/physics/sfe/ZEUS_PUBLIC/public_plots/rosenbluth.eps`

[18] J. Kretzschmar, to appear in the DIS 2009 workshop proceedings.